Available online at www.sciencedirect.com
SCIENCE DIRECT
Polymer 46 (2005) 12677–12681
polymer
www.elsevier.com/locate/polymer

Imaging of local vibratory and non-vibratory domains in ferroelectric P(VDF-TrFE) films

GuoDong Zhu [a,*], Jing Xu [b], XueJian Yan [a], Jie Li [b], Li Zhang [a], ZhiGang Zeng [a], Miao Shen [a]

[a] Department of Materials Science, Fudan University, 220 Handan Road, Shanghai 200433, China
[b] Department of Physics, Tongji University, 1239 Siping Road, Shanghai 200092, China

Received 30 August 2005; received in revised form 8 October 2005; accepted 25 October 2005
Available online 11 November 2005

Abstract

In this paper we studied the distribution of local piezoelectricity in P(VDF-TrFE) ferroelectric films, and observed the coexistence of vibratory and non-vibratory domains. In all such experiments, we could observe the coexistence of in-phase vibratory domains with non-vibratory ones, or opposite-phase vibratory domains with non-vibratory ones, but no coexistence of in-phase domains with opposite-phase ones could be obtained. The origin of vibratory and non-vibratory domains was also discussed.

Keywords: AFM; Piezoelectricity; P(VDF-TrFE)

1. Introduction

Ferroelectric polymers such as poly(vinylidene fluoride) (PVDF) and its copolymer P(VDF-TrFE) have been well studied because of their applicability to transducers, sensors, actuators, and potential ultra-high-density data storage [1–3]. With this background, elucidation of ferroelectric domain structures and the origin of ferroelectricity of these polymers is one of the important issues in terms of academic and practical points of view.

PVDF and its copolymers are semi-crystalline with coexistence of crystalline phase and amorphous phase. Traditional researches are mostly based on macro-scale, and these macroscopic measurements can only be the complicated average of ferroelectricity and piezoelectricity of amorphous phases and crystalline phases embedded in amorphous ones. To have an understanding of the mechanisms behind piezoelectricity and ferroelectricity, it is essential to study local ferroelectricity and piezoelectricity of amorphous phases and crystalline phases, respectively.

Recently, scanning probe microscopy techniques have been utilized to investigate local structures and electrical properties of P(VDF-TrFE) thin films. Güthner and Dransfeld demonstrated the possibility to control and image local polarized domains on P(VDF-TrFE) thin films by using atomic force microscope (AFM) [4]; Matsushige et al. studied local piezoelectric properties of PVDF and P(VDF-TrFE) thin films prepared by spin-coating and vacuum-deposition methods whose thickness were on the order of several nanometers to several tens of nanometers [5,6]; Bune et al. succeeded in preparing two-monolayer copolymer film by Langmuir-Brodgett (LB) method and discovered two-dimensional ferroelectricity [7]. In spite of such impressive experimental results on organic ferroelectric films reported so far, their ferroelectric switching mechanisms are not elucidated yet.

In this paper, based on the excellent nanometer-scale resolution of AFM and the local measurement technique of piezoelectricity [8], we studied the distribution of local piezoelectricity in well-grown P(VDF-TrFE) films and visualized vibratory domains from non-vibratory ones. The origin of vibratory and non-vibratory domains was also discussed.

2. Experimental

An aluminium electrode with a thickness of about 50 nm was firstly deposited onto a flat cleaned glass substrate. Copolymer films were spin-coated from a 7.5% by weight solution of 60/40 P(VDF-TrFE) in butanone onto the top of this Al-electrode, and the film was annealed at 145 °C for 6 h to increase its crystallinity. The thickness of such films was about 0.8 μm. Finally a 30 nm-thick gold electrode was evaporated

* Corresponding author.
E-mail address: gawdon@hotmail.com (G.D. Zhu).

0032-3861/$ - see front matter © 2005 Elsevier Ltd. All rights reserved.
doi:10.1016/j.polymer.2005.10.118

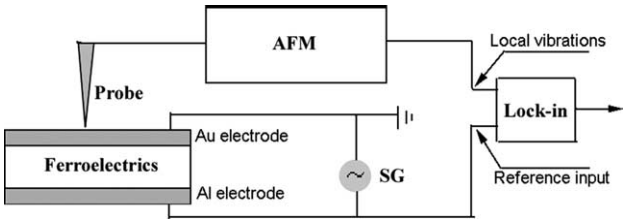

Fig. 1. Schematic diagram for local measurement technique of piezoelectricity.

onto the copolymer film. The coercive filed E_c of P(VDF-TrFE) films was about 50 MV/m, and then the corresponding coercive voltage of these films used in this paper was about 40 V. With this sandwich configuration a series of electrical experiments were performed.

Fig. 1 showed the schematic diagram for local measurement technique of piezoelectricity. AFM (NanoScope IIIa, Veeco Ins.) scanned on sample surface with a slow rate. A signal generator SG simultaneously outputted a driving voltage V_d with an amplitude of 10 V and a much higher frequency up to 400 Hz onto sample. The voltage-excited surface vibrations, detected by AFM, were inputted into a lock-in amplifier as an input signal, and simultaneously the driving voltage V_d was also inputted into this lock-in amplifier as a reference signal. The magnitude of lock-in output denoted the amplitude of local vibrations, and the phase of lock-in output would denote the dependence of surface vibrations on the driving voltage. A positive lock-in output indicated a positively linear dependence of surface vibrations on the driving signal, while a negative output indicated a negatively linear dependence of local vibrations on the driving voltage (that is to say, surface vibrations were in opposite phase with respect to the driving voltage). Thus we could study the space distribution of local piezoelectricity.

During the whole measurements of local piezoelectricity, Au-electrode was always grounded, and the driving voltage V_d or/and poling voltage V_p was applied to Al-electrode. In this paper we would call a polarized state as a positively polarized state, when Al-electrode was negatively biased by poling voltage V_p; and call a state as a negatively polarized state when Al-electrode was positively biased.

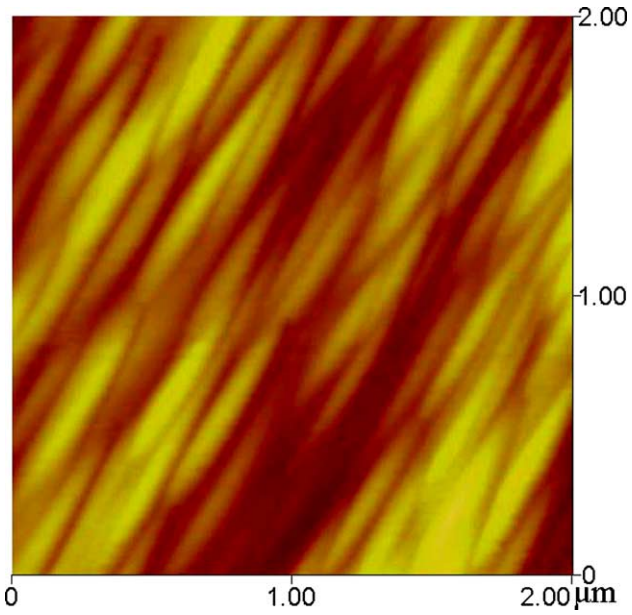

Fig. 2. AFM morphology of poled well-grown P(VDF-TrFE) film.

3. Results

The copolymer films were pre-polarized. AFM morphology of this polarized well-grown P(VDF-TrFE) film was shown in Fig. 2. Film surface was covered with long sausage-like domains with uniform orientation.

3.1. Distribution of local piezoelectricity

Firstly we studied space distribution of local piezoelectricity on one dimension. AFM's probe scanned along one-dimensional direction. The scan was performed rather slowly, with a scan rate of 0.1 Hz, across a scan size of about 200 nm. A triangular driving voltage V_d (400 Hz, 20 V_{p-p}) was always applied during the course of AFM scanning.

Fig. 3 showed one result of such experiments, in which the X-axis indicated the scan scale of AFM, and the Y-axis indicated the output voltage of lock-in amplifier. When AFM began its forward scan (the forward scan direction was marked by an arrow at the top of Fig. 3, or from point A to point D), a Dc poling voltage V_p of +75 V was always applied to Al electrode and the sample was in negatively polarized state. At this state lock-in amplifier had a positive-voltage output, which indicated an in-phase vibration with respect to the driving voltage V_d. The whole recorded lock-in output during the forward scan lied in the upper curve in Fig. 3. When the forward scan had finished (at point D in Fig. 3) and the probe was going to start its backward scan (backward scan direction was also marked by an arrow at the bottom of Fig. 3, or from point E to point H), a polarization reversal occurred by replacing the positive V_p of +75 V with a negative poling voltage of −75 V, and now the sample was in positively polarized state. The vibratory property on film surface was

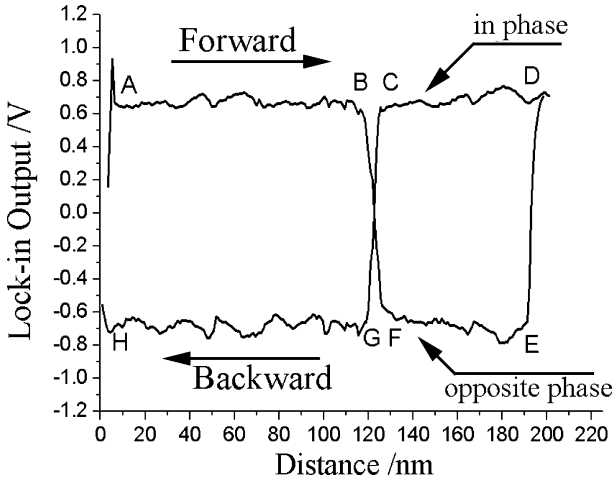

Fig. 3. Distribution of local piezoelectricity along one-dimensional direction.

immediately reversed from in-phase to opposite-phase vibrations, and the lock-in output turned from positive to negative voltage (see the bottom curve in Fig. 3).

The recorded curves in Fig. 3 showed that lock-in output kept rather flat during the whole scan scale of 200 nm, except one local region. Between point B (G) and point C (F) vibratory signals suddenly dropped down to zero, that is to say, whether the sample was in positively or negatively polarized state, the surface at this local region did not vibrate, although driving voltage V_d was still applied to this local region. This local region was regarded as a 'non-vibratory domain', while the other local regions was called 'vibratory domains'. The dimension of this non-vibratory domain was only about 8 nm.

In all such experiments, we observed the coexistence of in-phase vibratory domains with non-vibratory domains, or opposite-phase vibratory domains with non-vibratory ones, but no coexistence of in-phase domains with opposite-phase domains could be detected.

The output of lock-in amplifier during backward scan was nearly a mirror image of the output during forward scan. The polarization reversal only changed the sign of the lock-in output, but its absolute value remained unchanged. This mirror image also illuminated that our local measurement technique had an excellent reproducibility.

3.2. Imaging of vibratory domains and non-vibratory domains

AFM scanned in two dimensions, and the output of lock-in amplifier was fed back into AFM system and was recorded by the software, thus we could visualize the vibratory domains from non-vibratory ones. Fig. 4(a) showed the AFM morphology (Fig. 4(a1)) and the simultaneously recorded imaging (Fig. 4(a2)) of vibratory domains and non-vibratory domains at the same local region. The sample was negatively pre-polarized, so the light regions in Fig. 4(a2) were corresponding to vibratory domains, while dark regions were corresponding to non-vibratory ones. Two vibratory domains with irregular shapes were imaged, and these two domains were separated by a non-vibratory domain. Fig. 4(b) displayed the profile analysis. Fig. 4(b2) clearly displayed two vibratory domains, between which was a non-vibratory domain. The distribution of vibratory and non-vibratory domains had no evident dependence on topography (See Fig. 4(b)).

4. Discussions

AFM is well known for its excellent lateral resolution down to an atomic scale. A non-vibratory domain with width of 8 nm has been obviously imaged in Fig. 3, which also illuminates the high resolution of our local measurement technique. The lamellar crystallites of P(VDF-TrFE) are known to be about several tens of nanometers thick [9], and considerably larger in the other two directions (by electron microscopy it has been found that the crystallites can have lateral size up to 3 μm [10]), and these crystallites are known to be oriented with their large dimensions perpendicular to the surface [11]. So the detected local vibrations, obtained by AFM's probe, are not averaged properties of several crystalline domains in the directions parallel to sample plane, but oscillations on a single domain surface. However, films in this paper are about 0.8 μm thick, so there would be several tens of crystalline domains in the direction normal to the film plane, that is to say, the observed local vibrations are the integrated results of many domains existing in film-thickness direction.

Fig. 3 shows the space distribution of local piezoelectricity, and we have observed the coexistence of vibratory domains with non-vibratory ones. From all our local experimental data, we observe the coexistence of in-phase vibratory domains and non-vibratory domains, or opposite-phase vibratory domains and non-vibratory domains, but no coexistence of in-phase and

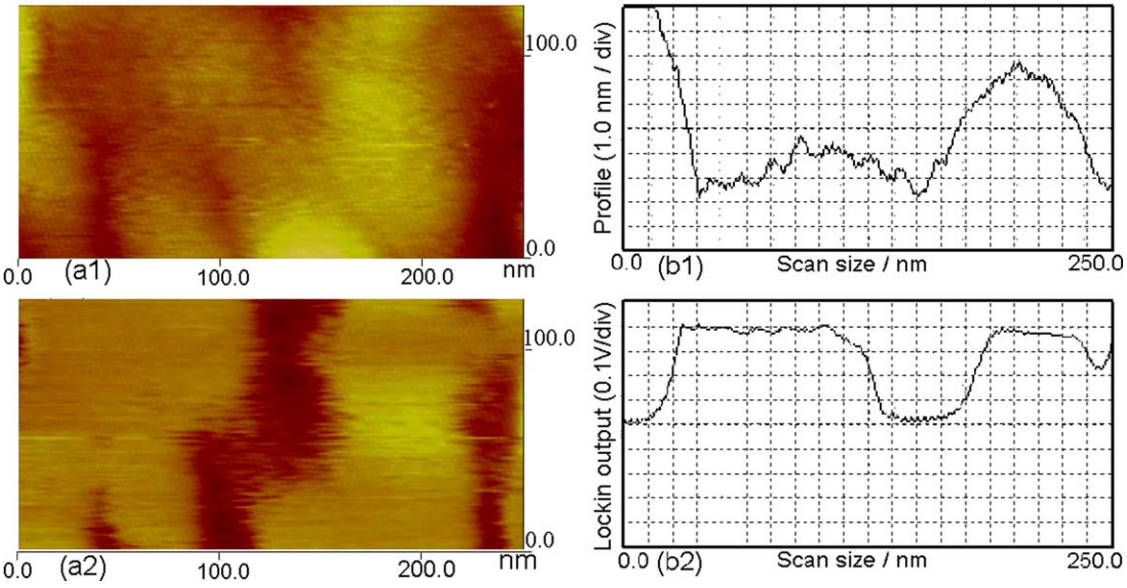

Fig. 4. Imaging of the local vibratory and non-vibratory domains in P(VDF-TrFE) films. (a) SPM morphology (a1) and simultaneously imaging (a2) of vibratory and non-vibratory domains. (b) Profile analysis of morphology (b1) and distribution (b2) of vibratory and non-vibratory domains.

opposite-phase vibratory domains can be detected. In our previous work [12], it has been proved that amorphous phase in P(VDF-TrFE) films can also be ferroelectric and piezoelectric, so this coexistence can not be explained only by the concepts of crystalline phase and amorphous phase, and those non-vibratory domains can not be simply attributed to amorphous phase.

We consider the possible combinations of ferroelectric domains in the direction of film thickness, which was shown in Fig. 5(a). In state A, all ferroelectric domains can be switched by poling voltages, which are regarded as 'active domains'. In state B and C, only part of domains can be switched and the others are restricted for some reason and can not be reversed by poling voltage, these restricted domains are defined as 'inactive domains'. In state C the total dipole moment for inactive domains is zero, while it is not zero in state B. In state D and E, all domains in the direction of film thickness are inactive and their net dipole moment is zero for state E or not zero for state D.

Fig. 5(b) indicates the possible lock-in output corresponding to these different combinations of domains in Fig. 5(a). (1) Domains in state A are all active and can be completely reversed by positive or negative poling voltage, so the corresponding lock-in output should be symmetrical for both polarized states, which is consistent with the situation observed in Fig. 3. (2) For state B, the net dipole moment for inactive domains is not zero, that is to say, although part of domains are active, the absolute values of spontaneous (or remnant) polarization should be asymmetrical for positively and negative polarized states. Macroscopic measurements have already approved that piezoelectric coefficient has a linear dependence on spontaneous polarization in ferroelectric polymers [13,14], so the corresponding lock-in output would also be asymmetrical (For the very situation shown in state B, the net dipole moment of inactive domains is downward, so the lock-in output in positively polarized state would be larger than that in negative state). This combination is contrary to the experimental results of symmetrical lock-in output shown in Fig. 3, so state B impossibly occurs in our experimental situation. (3) For state C, only the active domains can contribute to spontaneous polarization and furthermore to local piezoelectricity, so lock-in outputs should also be symmetrical for both polarized states. However, because of fewer active domains in this state than those in state A, spontaneous polarization would be smaller, so voltage-induced local vibrations would also be weaker and the absolute values of lock-in output in both polarized states would be smaller than those exhibited in state A. The experimental curves shown in Fig. 3 are rather flat, but still have some fluctuations of about 20%. These fluctuations can be caused just by experiment error or by the situation shown in state C. In this paper we can not judge which factor should have the primary contribution to these fluctuations. (4) For state D, whether in positively or in negatively polarized state, poling voltages can not change the orientations of those inactive domains, so lock-in output should have the same value, which differs from the observed curves in Fig. 3. (5) For state E, domains are disorderedly oriented and the spontaneous polarizations caused by these disordered domains counteract each other, so in either polarized states, no local vibrations can be detected in this state, consistent with the observed non-vibratory domains in Fig. 3.

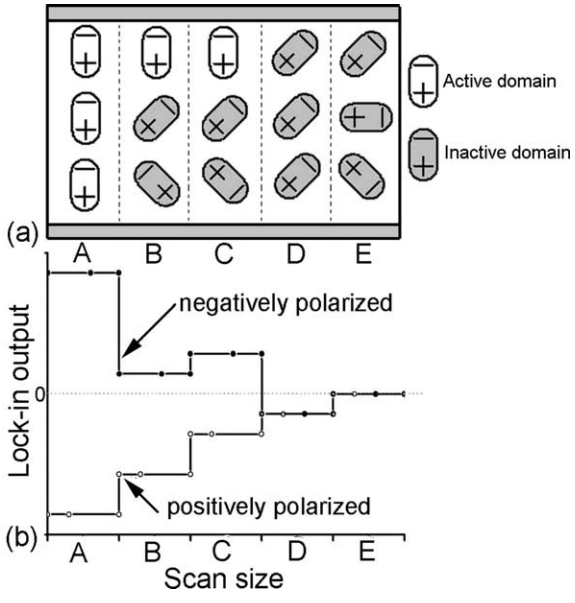

Fig. 5. Possible combinations (a) of ferroelectric domains in the direction of film thickness and the corresponding lock-in output (b) in positively and negatively polarized states.

From the analysis above, we believed that the observed vibratory domains in Fig. 3 should be attributed to state A in Fig. 5(a), and perhaps state C can also has some contribution, while non-vibratory domains should be attributed to inactive domains with disordered orientations in state E.

In the study of polarization fatigue in inorganic ferroelectrics [15], non-switchable domains are also be observed in inorganic ferroelectrics after frequent switching process, and this ferroelectric fatigue is attributed to the inactive domains pinned by space charges. The influence of trapped charges on switching process in ferroelectric polymers is also abundantly reported [16,17]. Based on these reported experimental facts, we believe it is trapped charges that lock the domain orientations and make them inactive even under the influence of poling voltage. But how these trapped charges work is still an open question.

To understand organic ferroelectricity and piezoelectricity, further work is necessary to prepare ultrathin films, which can be as thin as several monolayers, and study the local electrical properties on the scale of veritable single domains.

5. Conclusion

Based on the excellent lateral resolution of AFM and the local measurement technique of piezoelectricity, we reported the study on local piezoelectric distribution in well-grown P(VDF-TrFE) ferroelectric films. Our work displayed the coexistence of vibratory and non-vibratory domains, and in all

such experiments, we observed the coexistence of in-phase vibratory and non-vibratory domains, or opposite-phase vibratory and non-vibratory domains, but no coexistence of in-phase and opposite-phase vibratory domains could be detected. The origin of vibratory and non-vibratory domains was also discussed.

References

[1] Kawai H. Jpn J Appl Phys 1969;8:975.
[2] Wang TT, Herbert JM, Glass AM, editors. The application of ferroelectric polymers. Glasgow: Blackie and Son; 1988.
[3] EL-Hami K, Hara M, Yamada H, Matsushige K. Ann Chim Sci Mat 2001; 26:217.
[4] Güuthner P, Dransfeld K. Appl Phys Lett 1992;61:1137.
[5] Chen XQ, Yamada H, Terai Y, Horiuchi T, Matsushige K, Weiss PS. Thin Solid Films 1999;353:259.
[6] Noda K, Ishida K, Kubono A, Horiuchi T, Yamada H, Matsushige K. J Appl Phys 2003;93:2866.
[7] Bune A, Fridkin VM, Durcharme S, Blinov LM, Palto SP, et al. Nature 1998;391:874.
[8] Birk H, Glatz-Reichenbach J, Li J, Schreck E, Dransfeld K. J Vac Sci Technol B 1991;9:1162.
[9] Koga K, Ohigashi H. J Appl Phys 1986;59:2142.
[10] Broadhurst MG, Davis GT, McKinney JE, Collines RE. J Appl Phys 1978;49:4992.
[11] Tajitsu Y, Ogura H, Chiba A, Furukawa T. Jpn J Appl Phys 1987;26:554.
[12] Li J, Baur C, Koslowski B, Dransfeld K. Physica B 1995;204:318.
[13] Furukawa T, Chen JX, Suzuki K, Takashina Y, Date M. J Appl Phys 1984; 56:829.
[14] Park C, Ounaies Z, Wise KE, Harrison JS. Polymer 2004;45:5417.
[15] Tagantsev AK, Stolichnov I, Colla EL, Setter N. J Appl Phys 2001;90: 1387.
[16] Sussner H, Dransfeld K. J Polym Sci, Part B: Polym Phys 1978;16:529.
[17] Eberle G, Schmidt H, Eisenmenger W. IEEE Trans Dielectr Electr Insul 1996;3:624.